DNA Damage and Apoptosis Induction in Cancer cells by Chemically Engineered Thiolated Riboflavin Gold Nanoassembly

Abhishek Sau[†], Sulagna Sanyal[‡,$], Kallol Bera[†,$], Sabyasachi Sen[‡,$], Amrit Krishna Mitra[ŧ,$], Uttam Pal[†,$], Prabal Kumar Chakraborty[#], Sayantan Ganguly[‡], Biswarup Satpati[±], Chandrima Das[‡,*] and Samita Basu[†*]

[†]Chemical Sciences Division, HBNI, [‡]Biophysics and Structural Genomics Division, [#]Crystallography and Molecular Biology Division, [±] Surface Physics and Material Science Division, Saha Institute of Nuclear Physics, Kolkata, India, 700064, [ŧ] Department of Chemistry, Government General Degree College, Singur, Hooghly, West Bengal, 712409, India

Table of Contents

Fig. S1	**Synthesis and Characterization of RfSH and RfS@AuNPs and NMR data**	**S1**
	Materials and Methods	**S2**
Fig. S2	**Absorption spectra of RfSH /Rf with CAuNP**	**S3**
Fig. S3	**Quantification of RfSH attachment per AuNP**	**S4**
Fig. S4	**Transmission Electron Microscopy (TEM) of Different Gold Nanoparticles.**	**S5**
Fig. S5	**Fluorescence Data**	**S6**
Fig. S6	**Study of time-resolved fluorescence**	**S7**
Fig. S7	**DNA Intercalation study: UV**	**S8**
Fig. S8	**Determination of Drug-DNA Binding Strength from Steady-State Emission Spectral Data.**	**S9**
Fig. S9	**Circular dichroism (CD) studies.**	**S10**
	Laser Flash photolysis: DNA Intercalation.	**S11**
Fig.S10	**Flow Cytometric Data (FACS) data.**	**S12**
Fig.S11	**Green Intensity analysis from confocal images**	
Fig.S12	**pH stability of RfS@AuNPs**	
Fig. S13	**Volcano Plot for Micro array Gene analysis**	**S13**
Fig. S14	**PANTHER analysis of cellular processes altered by RfS@AuNPs treatment.**	

S1.a. Synthesis of Rf-OTs: A 500-mL, three-necked, round-bottomed flask fitted with a stirrer and a thermometer is charged with 200 mL of pyridine and 18.81 g (0.05 mol) of Riboflavin (Rf) in 200 mL of DMSO. The solution is stirred and chilled to 0°C and then 9.53 g (0.05 mol) of freshly recrystallized p-toluenesulfonyl chloride is added in portions over a 20-min period. The reaction mixture is allowed to attain room temperature and is stirred for 16 H. The mixture is re-cooled to 0°C and poured into 100 mL of concentrated hydrochloric acid in 500 mL of ice water. The aqueous layer is extracted with 100 mL of DCM and the combined organic layers are washed with two 60-mL portions of brine, dried over magnesium sulphate and concentrated by rotary evaporation to yield 10.2 g of a light yellow solid of **Rf-OTs**.

S1.b. Synthesis of RfSH: Rf-OTs, 10.61 g , 0.02 mol is dissolved in ether (100.0 ml) by continuous stirring and then 1,2-dithiane (2 g, 0.02 mol) is added in drop wise manner. The reaction mixture is stirred for 24 H in presence of catalytic amount of NaI (0.003 g, 0.00002 mol) under room temperature. The dark yellow product is purified using column chromatography and used as **RfSH**. The solid product is separated out and then crystallized in hot ethanol-water mixture that produces a pale yellow coloured solid (m.p.195 °C) of **RfSH** (~39%).

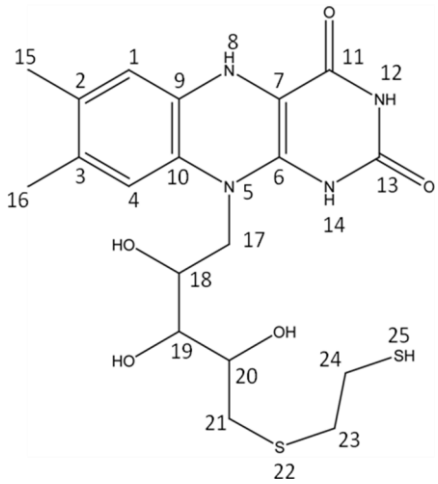

^{1}H NMR (300 MHz, DMSO-d6) δ, ppm= 11.34 (s, 1H, N12-H), 7.92 (s,1H, Ar-C1-H), 7.88 (s,1H, Ar-C4-H), 5.15 (s, N14-H), 4.59 (s, N8-H), 4.93, 4.90, 4.87, 4.8 (m, 1H, 1H, C18, 20-H), 4.80, 4.79 (d, 2H, C17-H), 4.63, 4.59 (d, 2H, C21-H), 3.47, 3.45, 3.43 (t, 1H, C19-H), 2.675, 2.671, 2.66, 2.64 (m, 2H, C24-H), 3.63 (s, 1H, 3-OH), 2.58 (s, 1H, S25-H). 2.57-2.50 (m, 2H,C23-H), 2.48 (s, 3H, C15-H), 2.40 (s, 3H, C16-H).

^{13}C NMR (75 MHz, DMSO-d6): 117.5(C1,C4), 135.7(C2), 136.7 (C3)150.8(C6), 146.1(C7), 132.1 (C9), 134.0(C10), 155.6 (C11), 160.0 (C13), 18.8 (C15,C16), 47.36 (C17), 63.4 (C18), 68.8(C19), 72.8 (C20), 73.6(C21), 40.3(C23), 38.2(C24).

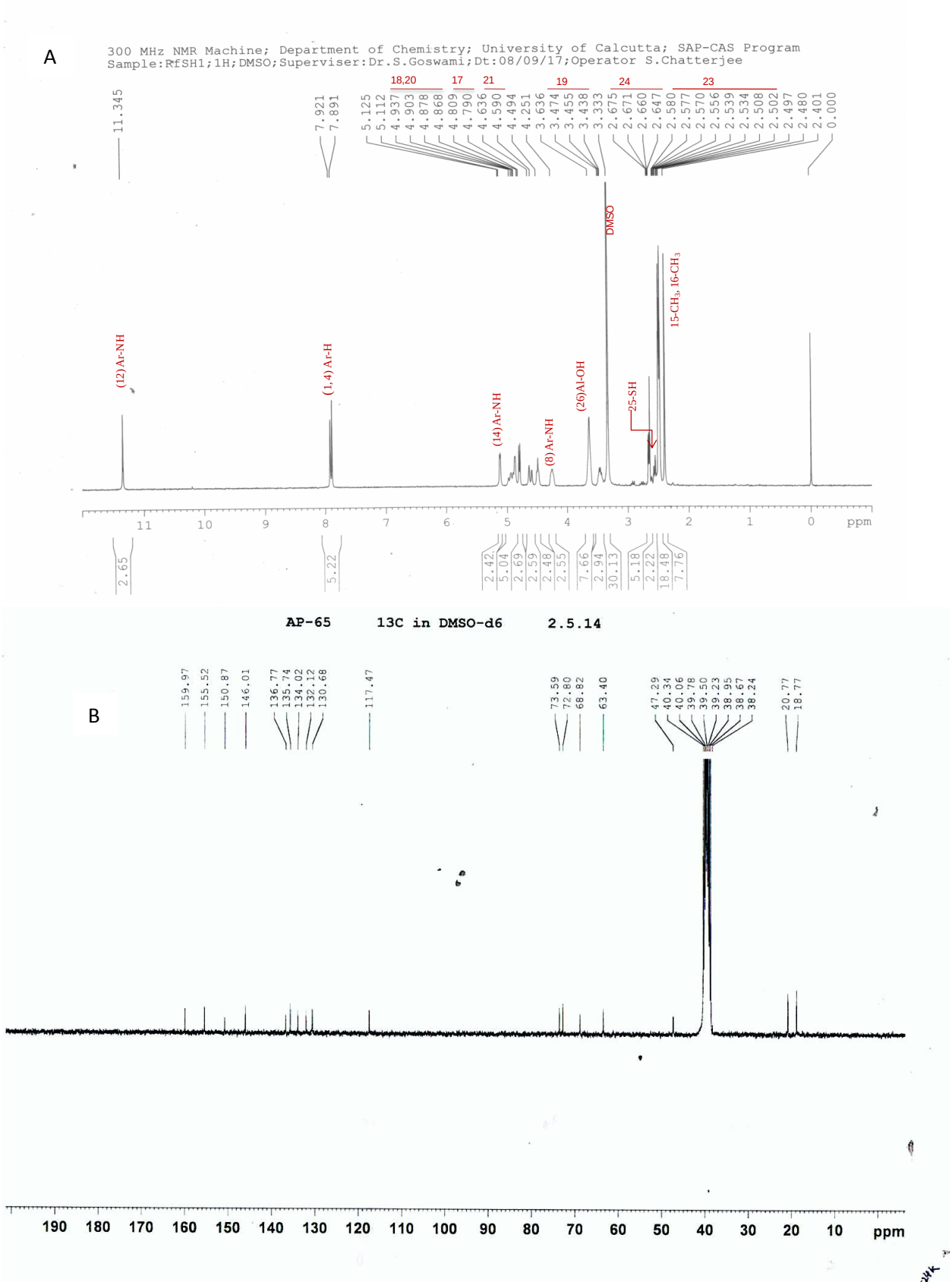
A
300 MHz NMR Machine; Department of Chemistry; University of Calcutta; SAP-CAS Program
Sample:RfSH1;1H;DMSO;Superviser:Dr.S.Goswami;Dt:08/09/17;Operator S.Chatterjee
(12)Ar-NH
(1,4)Ar-H
(14)Ar-NH
(8)Ar-NH
(26)Al-OH
25-SH
DMSO
15-CH3, 16-CH3
ppm
B
AP-65 13C in DMSO-d6 2.5.14
ppm

C

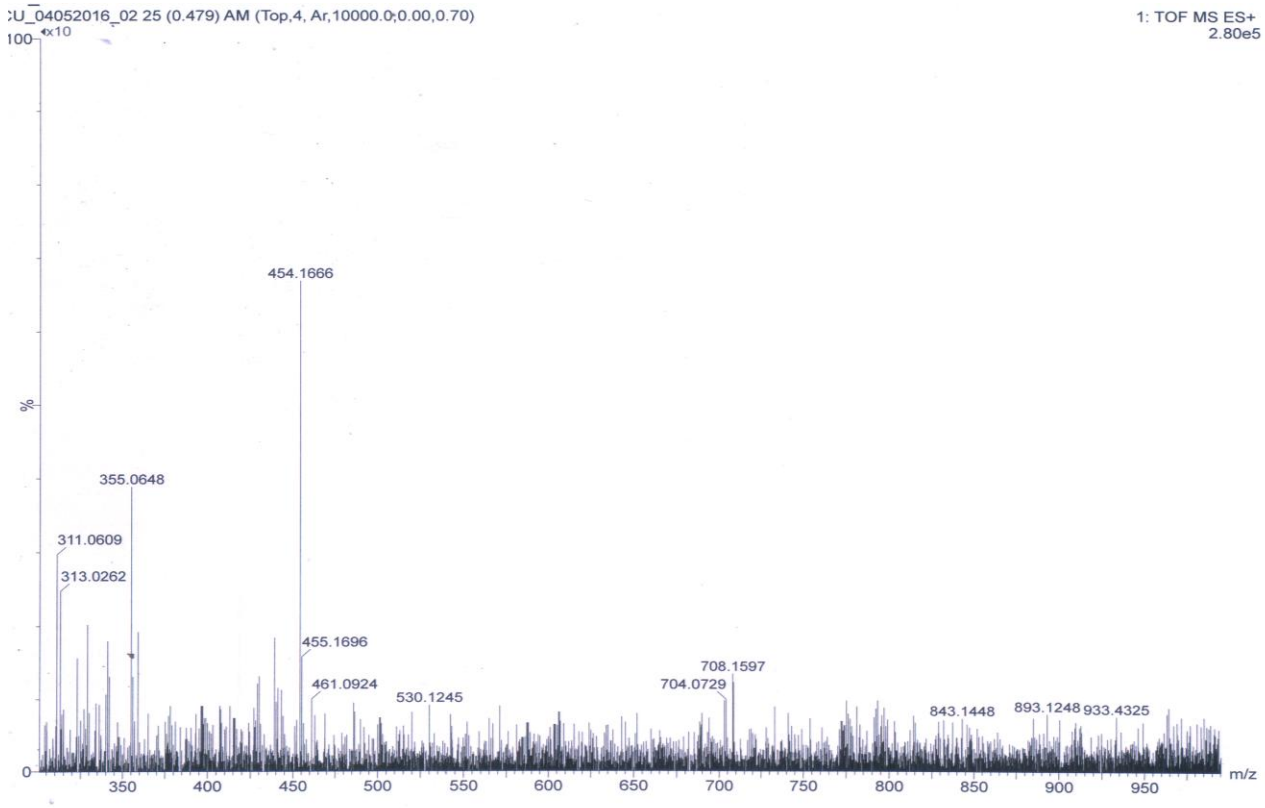

FigS1: (A) **^{1}H** and (B) **^{13}C** NMR spectra of **RfSH.** (C) ESI mass spectrum of **RfSH.**

m/z obtained for **RfSH** is : 454.16 [Exact mass 454.13]

S1.c. Preparation of citrate capped gold nanoparticles (CAuNPs): (Turkevich et al., 1951)

To a aqueous solution of $HAuCl_4$, $3H_2O$ (1M, 0.5 ml), autoclaved Millipore water (18.5 ml) is added and boiled for 2 minutes. To this boiling yellow solution Trisodiumcitrate (10^{-2}M, 0.5ml) is added drop wise. The color of the previous yellow solution of gold chloride turned into wine red. The Plasmon of the prepared gold sol is measured using absorption spectrophotometer (λ_{max}= 525nm).

S1.d. Preparation of RfS@AuNPs:

Aqueous solution of **RfSH** (5×10^{-4} M) is mixed with 1 nM **CAuNPs** in 1:4 ratio. Resulting solution is kept for ~ 4 H and centrifuged (at 4000 rpm) for 90 minutes. This process is repeated thrice. The bottom part is collected, redispersed in water and used as **RfS@AuNPs** for experiments. The concentration of **RfS@AuNPs** used for cell treatment is 0.5 nM .

S1.e. Preparation of Rf@AuNPs:

Aqueous solution of **Rf** (5×10^{-4} M) is mixed with 1 nM **CAuNPs** in 1:4 ratio. Resulting solution is kept for ~ 4 H and centrifuged (at 4000 rpm) for 90 minutes. This process is repeated thrice. The bottom part is collected, redispersed in water and used as **Rf@AuNPs** for each experimental step. The concentration of **Rf@AuNPs** used for cell treatment is 0.5 nM .

S2. Materials and Methods:

S2.a. Reagents and General Methods

All the chemicals and solvents required for syntheses of the thiol derivative of Riboflavin are of analytical grade. We have purchased 7,8-Dimethyl-10-[(2S,3S,4R)-2,3,4,5-Tetrahydroxypentyl]benzopteridine-2,4-dione (Riboflavin), 1,2-Ethanedithiol, from Aldrich Chemical Co., highly polymerized calf thymus DNA (CT-DNA) from Sisco Research Laboratory, India, and tris buffer, sodium chloride and hydrochloric acid (AR) from Merck and used without further purification. Triple distilled water has been used for the preparation of all the aqueous solutions. Solvents required for syntheses and spectroscopic studies have been purchased from SRL, India and Spectrochem, India respectively. $HAuCl_4 3H_2O$, trisodiumcitrate has been procured from Sigma. All the solvents have been purchased from commercial sources and distilled. Triple distilled deionized water has been used for all the experiments.

S2.b. Absorption and fluorescent measurements:

Steady-state absorption and fluorescence spectra of **Rf** are recorded by using JASCO V-650 absorption spectrophotometer and Spex Fluoromax-3 Spectro-fluorimeter respectively using a 1.0 cm path length quartz cuvette. For a given sample, the wavelength at which absorbance is maximum (λ_{max}) is used as excitation wavelength for corresponding emission scan.

The fluorescence lifetime measurement is performed using a picosecond pulsed diode laser based TCSPC fluorescence spectrometer with λ_{ex} = 377 nm and MCP-PMT as a detector. The emission from the samples is collected at right angle to the direction of the excitation beam maintaining magic angle polarization (54.7•) with a band pass of 2 nm. The full width at half maximum (FWHM) of the instrument response function is 270 ps and the resolution is 28 ps per channel. The data are fitted to exponential functions after deconvolution of the instrument response function by an iterative reconvolution technique using data analysis software in which reduced χ^2 and weighted residuals serve as parameters for better fit. All the steady-state and time-resolved measurements are performed at room temperature (298 K).

S2.c. Laser-flash photolysis:

Transient intermediates are generated with third harmonic (355 nm) output of nanosecond flash photolysis set-up (Applied Photophysics) containing Nd:YAG Laser (Lab series, Model Lab 150, Spectra Physics). A full width half maximum of the exciting laser is ~8 ns. Transient species in solution are detected through absorption of light from a pulsed xenon lamp (150 W) at right angle to the laser beam. The wavelength from the probe beam is dispersed with a monochromatic and detected with a photomultiplier detector (R928). The photomultiplier output is fed into an Agilent Infiniium oscilloscope (DSO8064A, 600 MHz, 4 Gs/s) and the data are transferred to a computer using IYONIX software. The detail of the experimental set-up is explained elsewhere. The software ORIGIN 8.0 is used for curve

fitting. The solid curves are obtained by connecting the points using B-spline option. The samples are deaerated by passing pure argon gas for 20 min prior to each experiment. No degradation of the sample is observed during the experiment.

S2.d. Transmission Electron Microscopy (TEM): TEM measurements have been carried out using an FEI, TECNAI G2F30, S-TWIN microscope operating at 300 kV equipped with a GATAN Orius SC1000B CCD camera. The diameter is analyzed manually by modeling each **AuNP** as a sphere, with statistical analysis using Image J software on populations of greater than 100 particles.

S2.e. Confocal microscopic data:

Hela cells are grown on coverslips in DMEM medium and treated with 0.5nM of different **drug@AuNP** (drug = **Rf/RfSH**) at different time points (6 H, 18 H and 24 H). After treatment the cells are fixed with 4% paraformaldehyde and washed with 1X PBS. Then slides are prepared with these cover slips using DAPI containing mounting media. Double stranded breaks in treated cells are detected by staining with anti **γ-H2AX antibody** (Abcam) at a dilution of 1:500.

For live cell experiment, Hela cells are cultured on 35 mm glass bottom petri dish (Genetix) in DMEM medium. Next day cells are treated with **RfS@AuNPs** at a concentration of 5μM for 6 H. After treatment the medium is changed freshly and live cell imaging is set up in an attached humid chamber (Tokai Hit, Japan) at 37^0C with 5% CO_2. Images are acquired at 30 min interval for next 18 H.

All microscopic images are acquired with Nikon's inverted confocal microscope where A1R+ confocal scanner head is mounted on Eclipse Ti-E microscope using 100X objective (oil immersion; NA 1.4). Nuclei are imaged using DNA binding dye DAPI with 405 nm laser. **RfS@AuNPs** are detected using 488 nm laser as the compound has excitation maximum at 444 nm. For detecting double stranded breaks the anti-γ-H2AX primary antibody is hybridized with secondary antibody conjugated with Alexa Fluor 594 (1:1000) and detected using 561 nm laser.

S2.f. Flow cytometry analysis

HeLa cells (untreated and **Rf@AuNPs**, **RfS@AuNPs** treated) are rinsed with PBS, trypsinized, pelleted, rinsed again in PBS, fixed in double volume of cold ethanol and stored at -20 °C for 2 H. Then the cells are rinsed with PBS, resuspended in 500 μl of PBS, treated with RNase (0.2 μg/μL at 37 °C for 30 minutes) followed by propidium iodide staining (0.05 μg/μL for 1 H at 37 °C) and subjected to flow cytometry on a FACS Calibur from BD Biosciences. Ten thousand events are collected in each run. Data are analyzed using Cell Quest software.

S3. Absorption spectra of RfSH /Rf in presence CAuNPs:

The citrate capped colloidal gold nanoparticles (**CAuNPs)** have characteristic wine red color originating from the coherent electron motion. The plasmon band at 525 nm in the UV–Vis spectrum is characteristic of gold nanoparticles as depicted in Fig S2. In ground state (5×10^{-6} M) riboflavin (**Rf**) and **RfSH** in water show two absorbance maxima in Fig S2 [368 nm and 444 nm]. With increase in concentration of nanoparticles (0.25→1.5nM), the absorbance (O.D.) gradually increases around 525 nm in case of **Rf** without formation of any new peak due to the lack of ground state interaction between **CAuNPs** and **Rf**. That is no significant change occurs in the surface plasmon of the [**CAuNPs**] in **Rf** solution. With increasing [**CAuNPs**] (0.25→1.5 nM) in a fixed **RfSH** solution the absorption maxium slightly shifts from 525 nm to 529 nm.

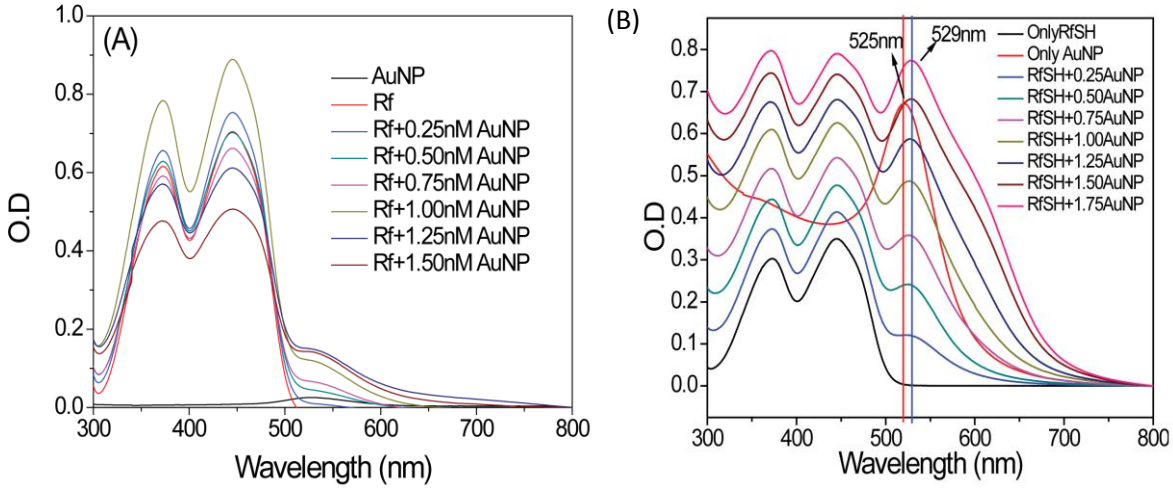

.

Figure S2: Absorption spectra of (A) **Rf** (5×10^{-6} M) in H_2O with increasing concentration **AuNPs** (0.25→1.5nM) in water.(B) Absorption spectra of **RfSH** (5×10^{-6}M) in H_2O with increasing concentration of **AuNPs** (0.25→1.75nM).

S4. Quantification of RfSH attachment per AuNP:

This experiment is performed to measure the amount of average drug molecule attached to an **AuNP**. The O.D of (Fig S3A) **Rf** (5×10^{-6}M) + **AuNP** (0.25nM) and (Fig S3B) **RfSH** (5×10^{-6}M) + **AuNP** (0.25 nM) in water are recorded first. Then the resulting solutions are centrifuged at 4500 rpm for 2 H. The upper part of the solution is then collected and O.D for the same is measured. The same process is performed for only **Rf** and **RfSH** (5×10^{-6} M) for negative control.

For both the cases the plasmon for the gold (525 nm) totally disappears after centrifugation and the O.D of the **Rf** (368 nm and 444 nm) deceases (~0.03) (fig. S3A) while for Rf-SH the decrease in O.D is 0.147 (~5 times as compared to **Rf**) (fig. S4B). No change is observed for the case of only **Rf** and **RfSH** (5×10^{-6}M) [Inst Fig.S3].

These observations indicate that **Rf** and **RfSH** get adhered on the surface of gold nanoparticles. As a result after centrifugation those conjugates (**Rf + AuNP** and **RfSH + AuNP**) get precipitated which is reflected through the absence of **AuNP** plasmon. Since the SH group has stronger affinity for **AuNP**, the amount of **RfSH** conjugated to **AuNP** is about 5 times greater as compared to **Rf**.

Again from the above experimental data (i.e. decrease in O.D) it is calculated that ~ 4680 number of **Rf** ligands and ~22800 number of **RfSH** ligands are attached with one gold nanoparticle (**AuNP** is assumed to be spherical with 20 nm average diameter proved latter by TEM image (Fig. S4).

Note: For **Rf and RfSH:** All the experiments with **Rf** and **RfSH** are reported here according to fluorophore concentration (in μM range).

For **Rf@AuNPs** and **RfS@AuNPs:** All the experiments with **Rf@AuNPs** and **RfS@AuNPs** are reported here according to nanoparticle concentration (in nM range)

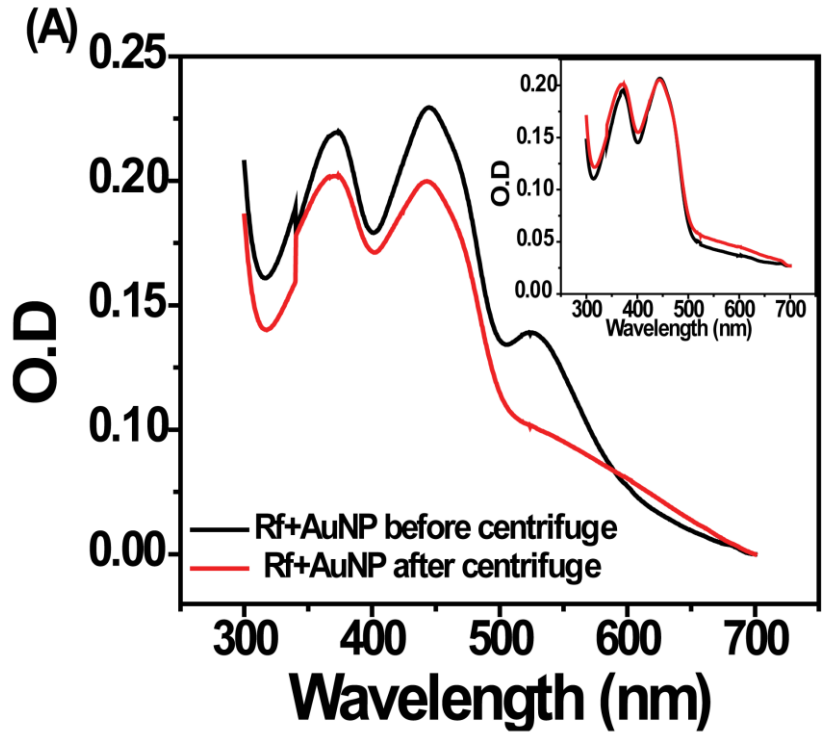

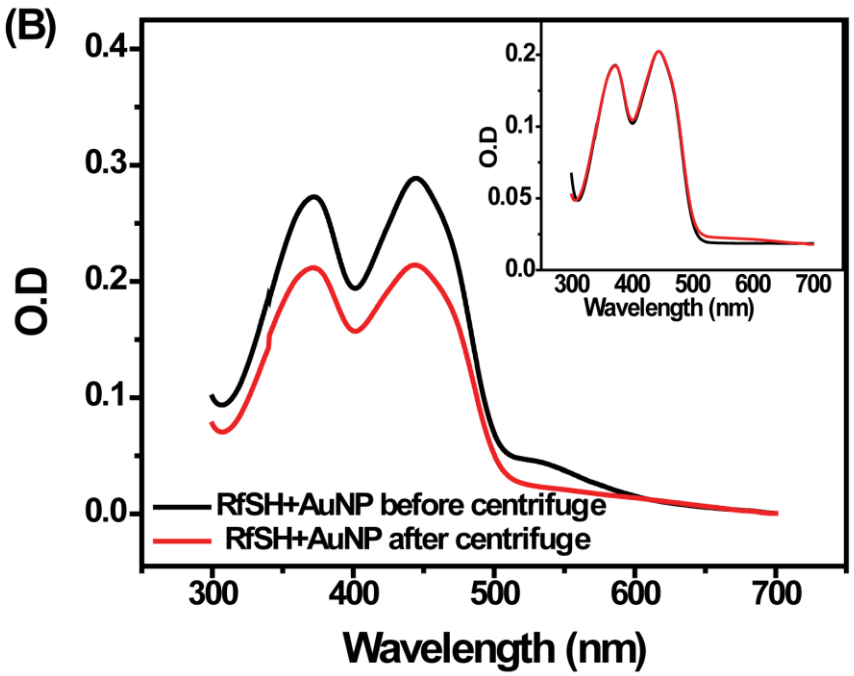

Figure S3: Absorption spectra of (A) **Rf** (5×10^{-6}M) (B) **RfSH** (5×10^{-6}M) in water with **CAuNPs** (0.25nM); (Inset spectra are of control i.e only **Rf** and **RfSH** without **CAuNP**) before and after centrifugation.

S5: Transmission Electron Microscopy (TEM) of Different Gold Nanoparticles.

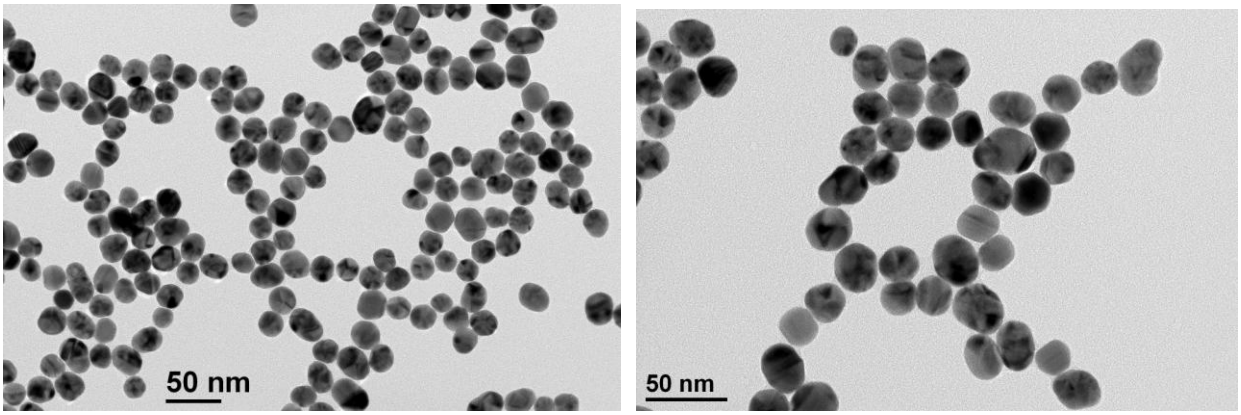

(A) **(B)**

Figure S4. Transmission electron micrographs of (A) **Rf@AuNPs** (B) Citrate capped gold nanoparticles (**CAuNPs**).

S6 Fluorescence Data:

The **AuNP** is non fluorescent. The fluorescence maximum (λ_{max}) of **Rf** is at 524 nm which is close to absorption wavelength of **AuNP** (λ_{max} = 525nm). Therefore, the emitted energy of **Rf** and **RfSH** might be getting absorbed by **AuNPs**. Therefore with the gradual increase of **AuNP** concentration (0.25→1.5 nM), this sort of energy transfer might be responsible for quenching of fluorescence intensity of **Rf**.

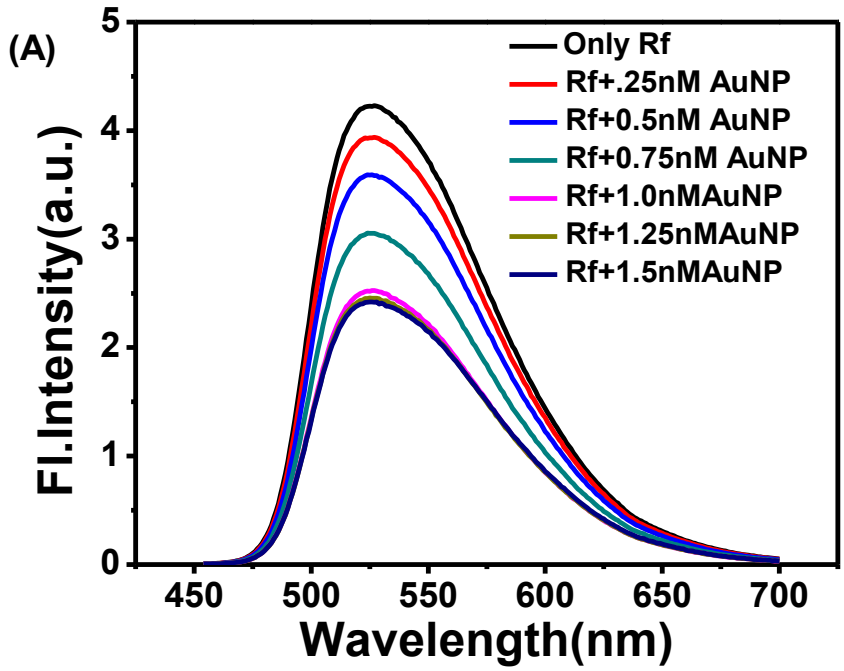

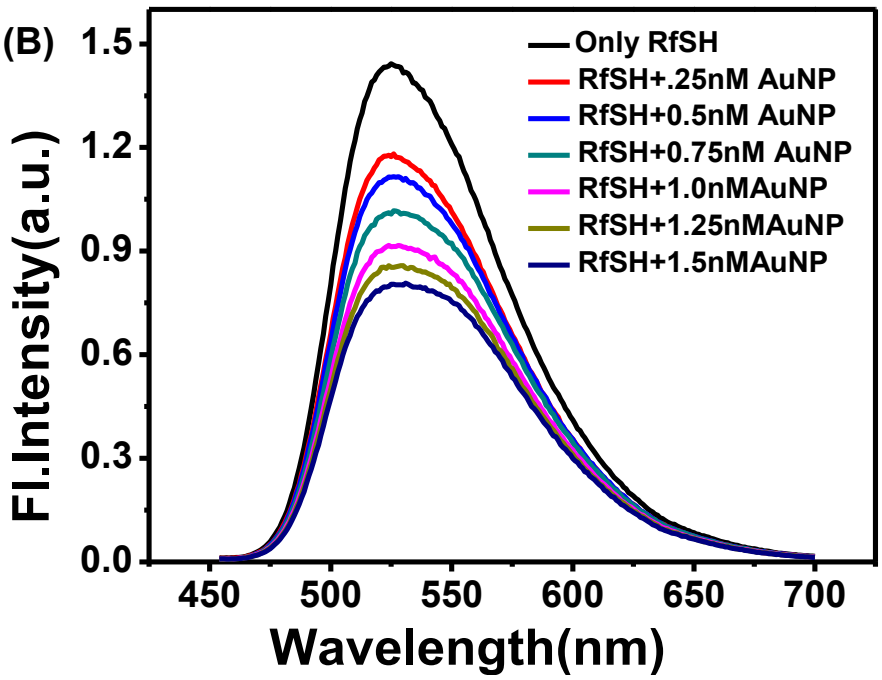

Figure S5: Fluorescence spectra of (A)**Rf** (5×10^{-6}M) (B) **RfSH** (5×10^{-6}M) in water with increasing concentration of **AuNPs** (0.25→1.5nM); (λ_{ex} = 444 nm)

S7 Study of time-resolved fluorescence:

The fluorescence lifetime of **Rf** is 4.73 ns and that of **RfSH** is 4.69 ns in aqueous medium. Moreover the lifetime of **Rf** and **RfSH** in aqueous medium remain unaltered with the addition of the gold nanoparticles (checked upto addition of 1nM). This reflects that the quenching in fluorescence emission is of static type and that is due to the formation of ground state complex of **Rf** or **RfSH** with C**AuNPs**.

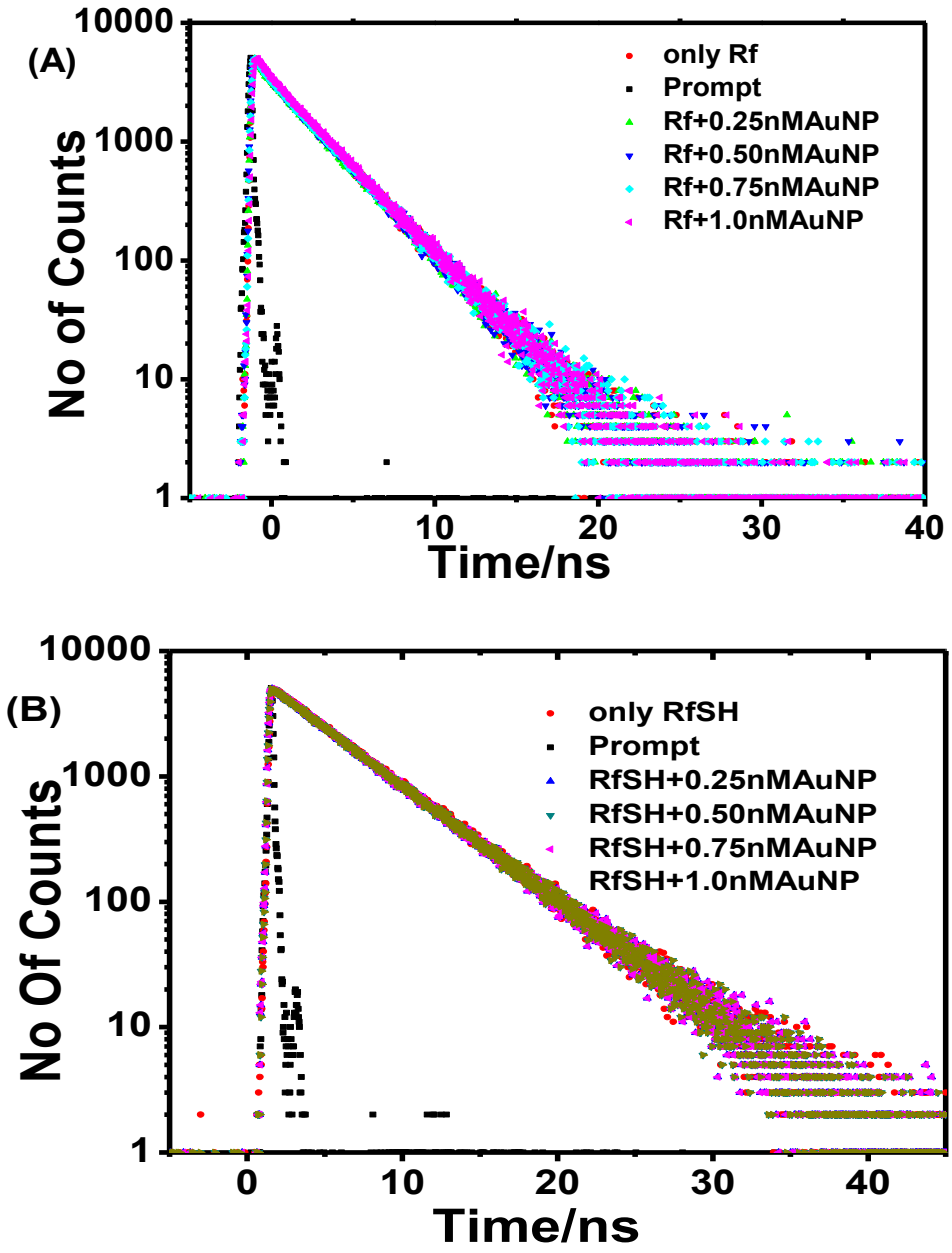

Figure S6: Time-resolved fluorescence decay spectra of (A) **Rf** (5×10^{-6}M) (B) **RfSH** (5×10^{-6}M) in water with gradual increase in concentrations of Gold nanoparticles (0.25→1nM) (λ_{ex} =377 nm)

S8: DNA Intercalation study:

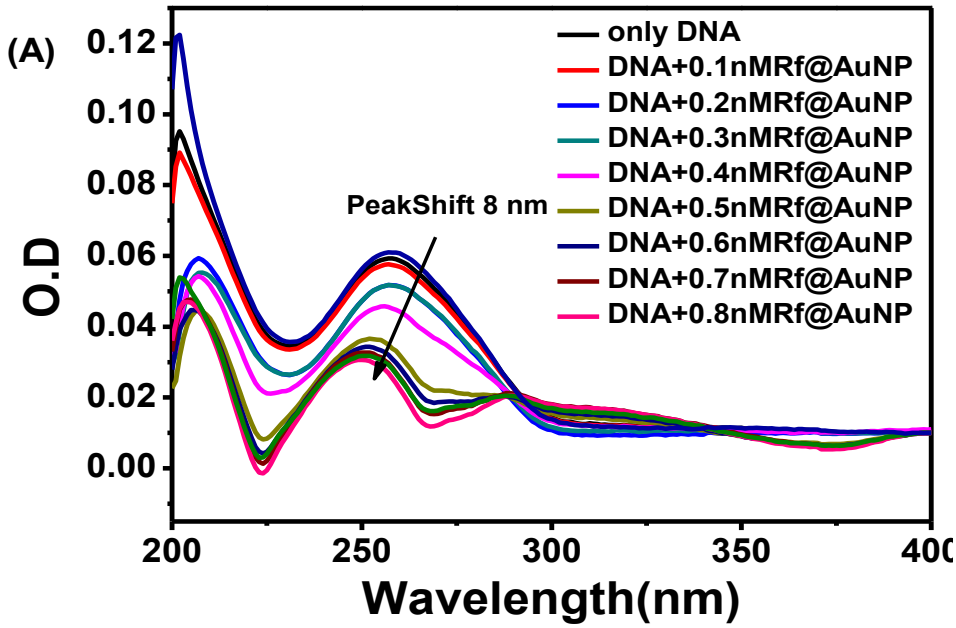
(A)
O.D
Wavelength(nm)
PeakShift 8 nm
only DNA
DNA+0.1nMRf@AuNP
DNA+0.2nMRf@AuNP
DNA+0.3nMRf@AuNP
DNA+0.4nMRf@AuNP
DNA+0.5nMRf@AuNP
DNA+0.6nMRf@AuNP
DNA+0.7nMRf@AuNP
DNA+0.8nMRf@AuNP

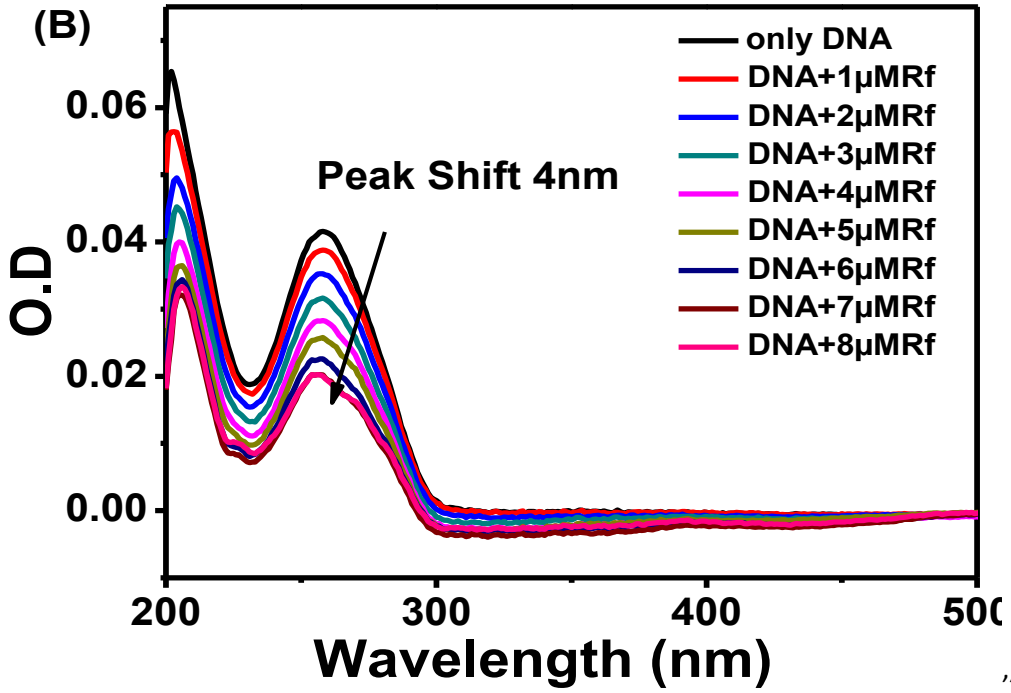
(B)
O.D
Wavelength (nm)
Peak Shift 4nm
only DNA
DNA+1μMRf
DNA+2μMRf
DNA+3μMRf
DNA+4μMRf
DNA+5μMRf
DNA+6μMRf
DNA+7μMRf
DNA+8μMRf

,,

(C)

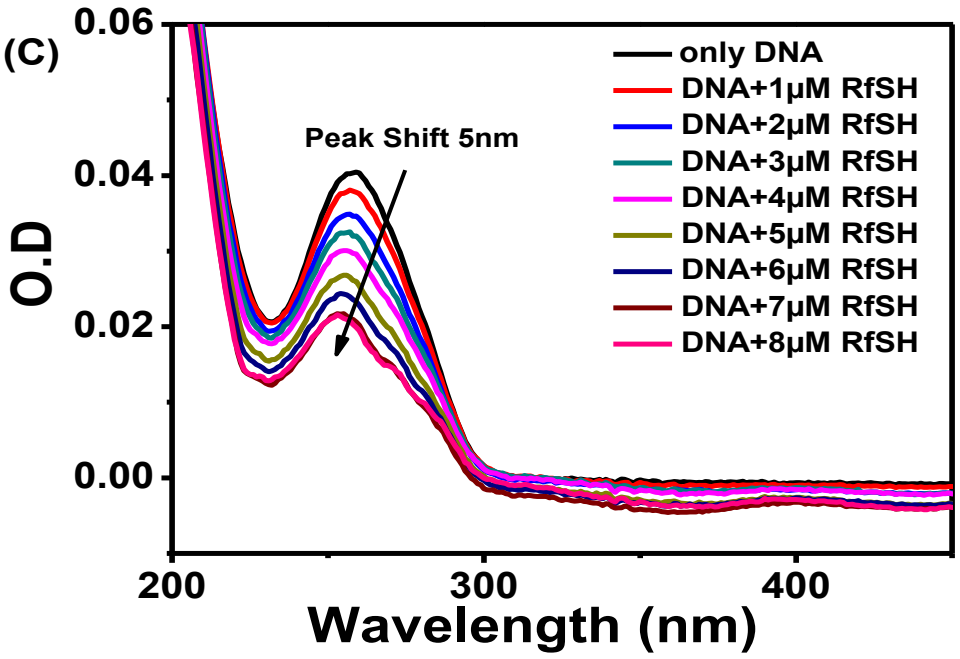

Figure S7: Absorption spectra of 10 μM DNA in Tris-buffer titrated with increasing concentration of (a) **Rf@AuNPs** (b) **Rf** (c) **RfSH**

S9. Determination of Drug-DNA Binding Strength from Steady-State Emission Spectral Data:

Calf Thymus - DNA (ct-DNA) itself is non fluorescent. Upon excitation (λ_{ex} = 444nm) isoalloxazine moiety of **Rf** emits at 525 nm. A regular enhancement of the fluorescence intensity with the gradual addition of ct-DNA is observed for both **Rf** and **RfSH**. With the addition of **AuNPs** the fluorescence emission intensity is quenched (shown in the Figure S7). With further addition of **AuNPs** the intensity of ct-DNA is again enhanced and even becomes greater than the intensity of **RfSH** alone. When isoalloxazine moiety of **Rf** intercalates DNA by stacking interaction among the base pairs, it enters in more constrained environment which prevents the nonradiative decay process, thus the enhanced fluorescence intensity is observed. Again the binding constant calculated for **RfS@AuNPs** ($\mathbf{K_b=1.1\times10^4}$) is greater than that for **RfSH** ($\mathbf{K_b=2.8\times10^3}$).

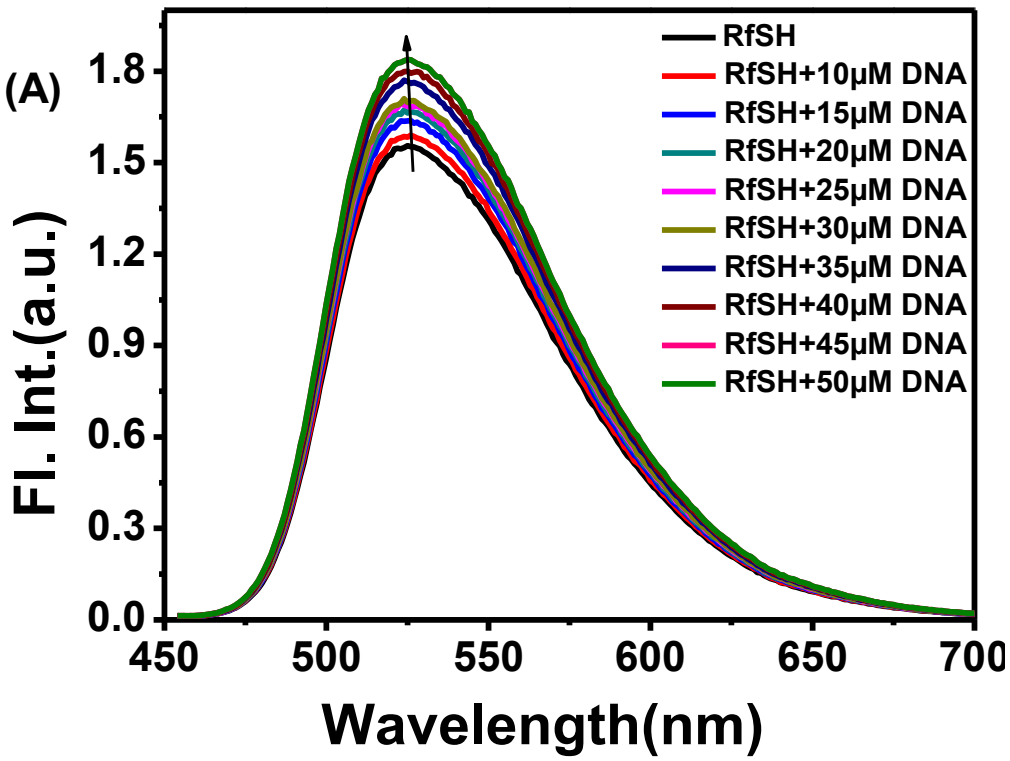
(A)
Fl. Int.(a.u.)
Wavelength(nm)
RfSH
RfSH+10μM DNA
RfSH+15μM DNA
RfSH+20μM DNA
RfSH+25μM DNA
RfSH+30μM DNA
RfSH+35μM DNA
RfSH+40μM DNA
RfSH+45μM DNA
RfSH+50μM DNA

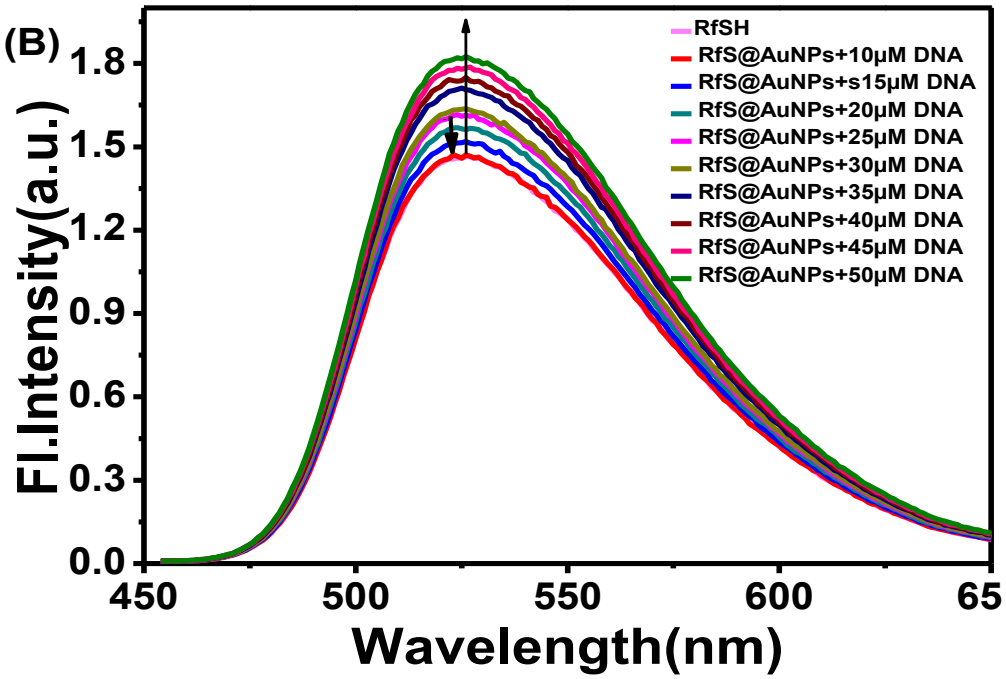
(B)
Fl.Intensity(a.u.)
Wavelength(nm)
RfSH
RfS@AuNPs+10μM DNA
RfS@AuNPs+s15μM DNA
RfS@AuNPs+20μM DNA
RfS@AuNPs+25μM DNA
RfS@AuNPs+30μM DNA
RfS@AuNPs+35μM DNA
RfS@AuNPs+40μM DNA
RfS@AuNPs+45μM DNA
RfS@AuNPs+50μM DNA

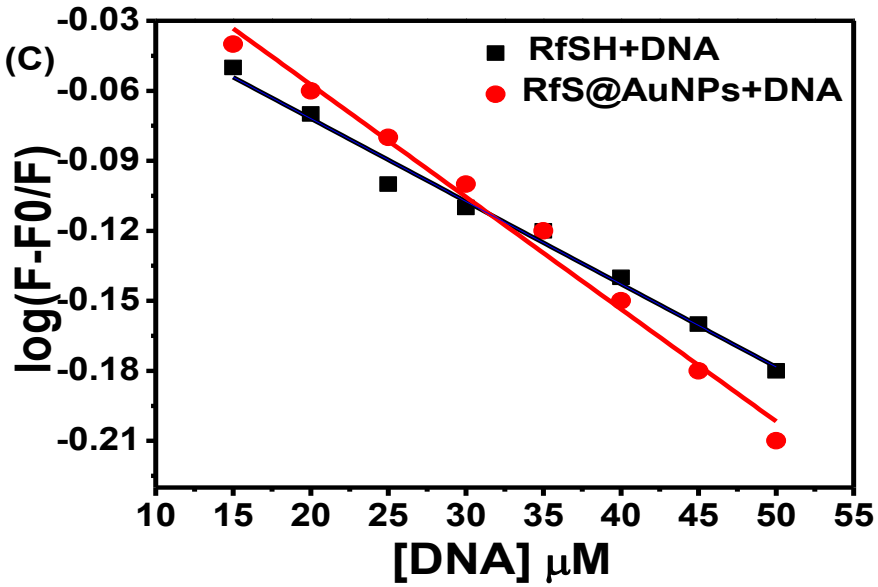

Figure S8: Emissions spectra of **(A) RfSH** (5×10^{-6} M) **(B)** (0.5nM) **RfS@AuNPs** (λ_{ex}=444nm) in tris-buffer with increasing concentration of ct-DNA (10→50 μM) (λ_{ex}=444nm).**(c)** Stern-Volmer plot for comparative enhancement of intensity and binding constant.

S10 .Circular dichroism (CD) studies:

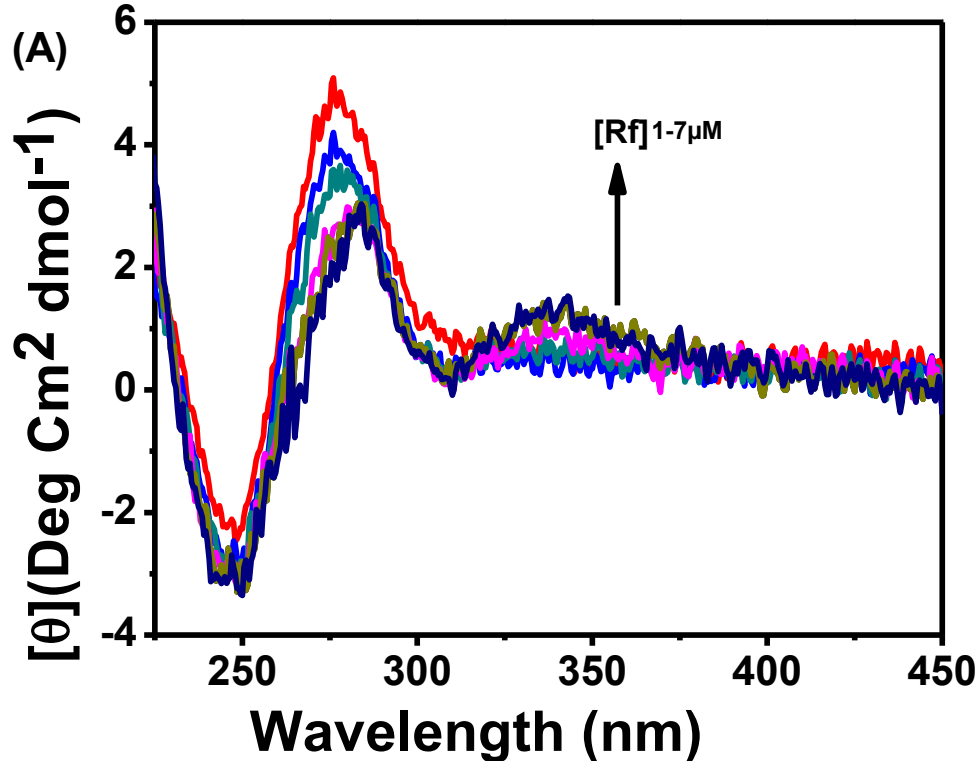

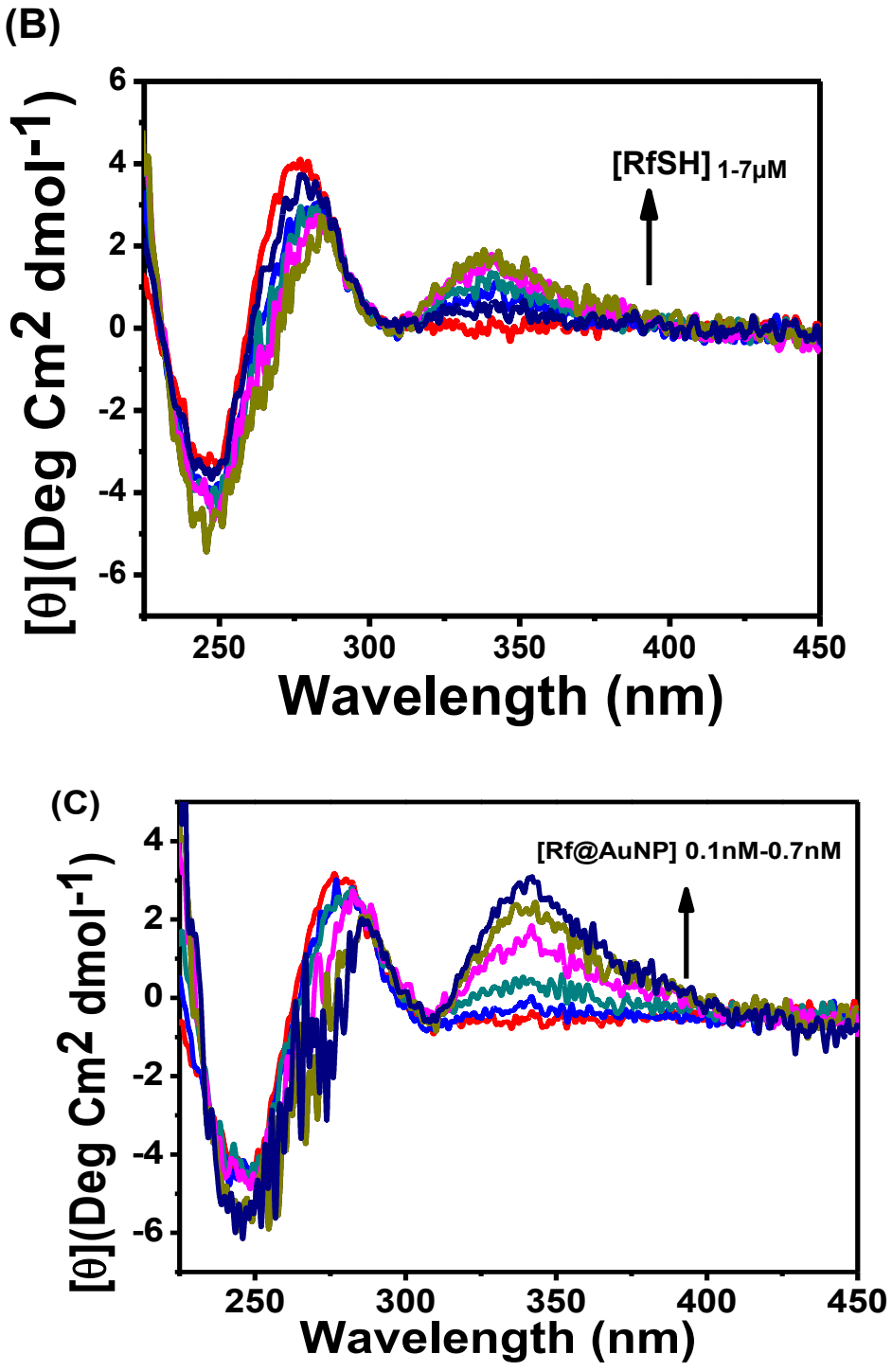

Figure S9: CD spectra of ct-DNA in Tris-buffer titrated with increasing concentration of (A) **Rf** (B) **RfSH** (1μM-7 μM) (C) **[Rf@AuNPs]** 0.1 nM-0.7 nM

S11. Laser Flash photolysis: DNA intercalation:

Triplet-triplet absorption of **RfS@AuNPs** shows peak around 360 nm and 530 nm in tris-buffer. It is observed that with the gradual addition of DNA the overall absorbance of **RfS@AuNPs** drops off along with a comparable decrease in the lifetime (T) of the transients at 360 nm and 530 nm from 2.8→2.1 μS and 2.9→2 μS respectively.This quenching occurs may be due to inaccessibility of isoalloxazine ring which is stacked within the DNA microenvironment. Again with the gradual increase in DNA concentration, the ground state interactions of **DNA** with **RfS@AuNPs** hamper the overall inter system cross over process. Hence triplet yield of **RfS@AuNPs** decreases. This data again support the hypotheses of ground state interaction between **RfS@AuNPs** and DNA**.**

S12: Flow cytometric Data (FACS) data:

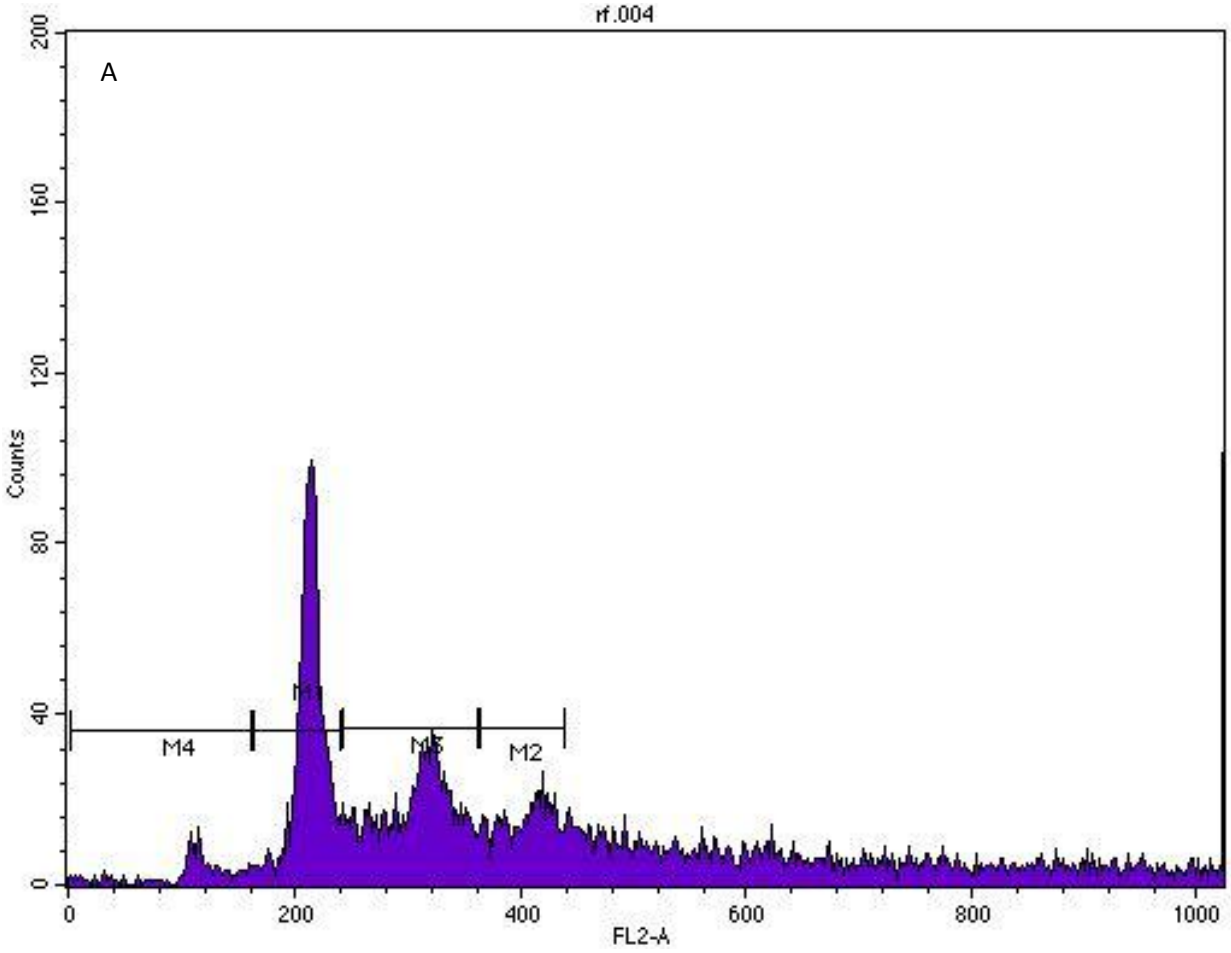

Figure S10A: Cell cycle affected by **Rf@AuNP**.

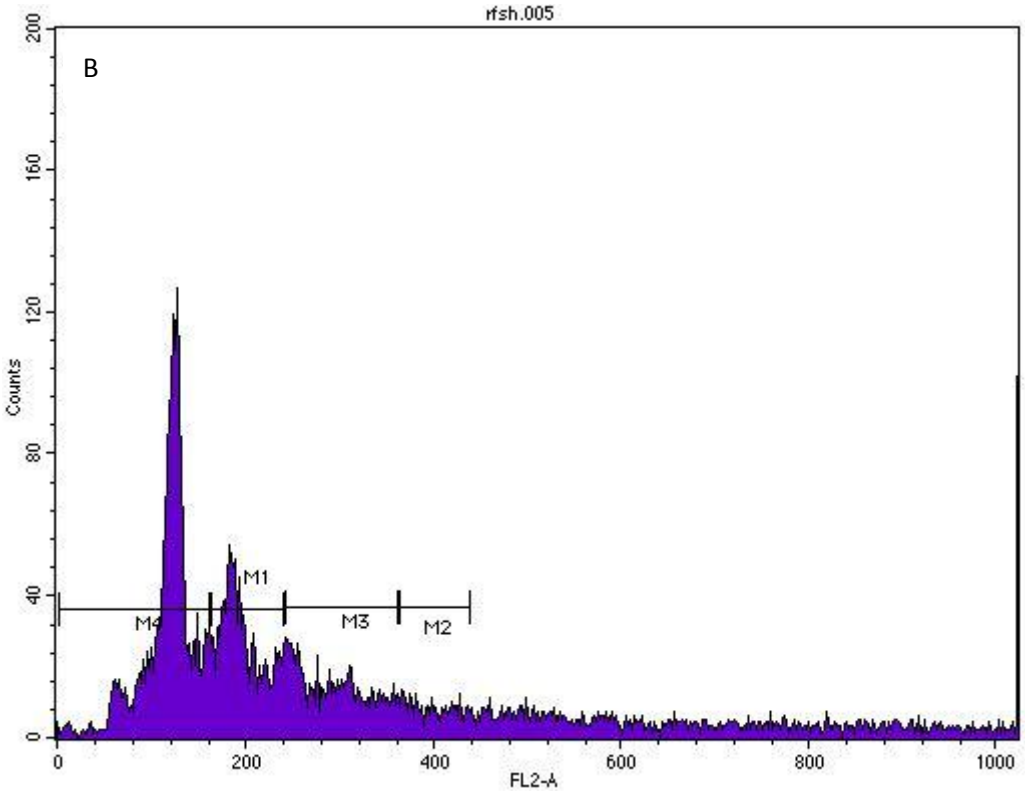

Figure S10B: Cell cycle affected by **RfS@AuNPs.**

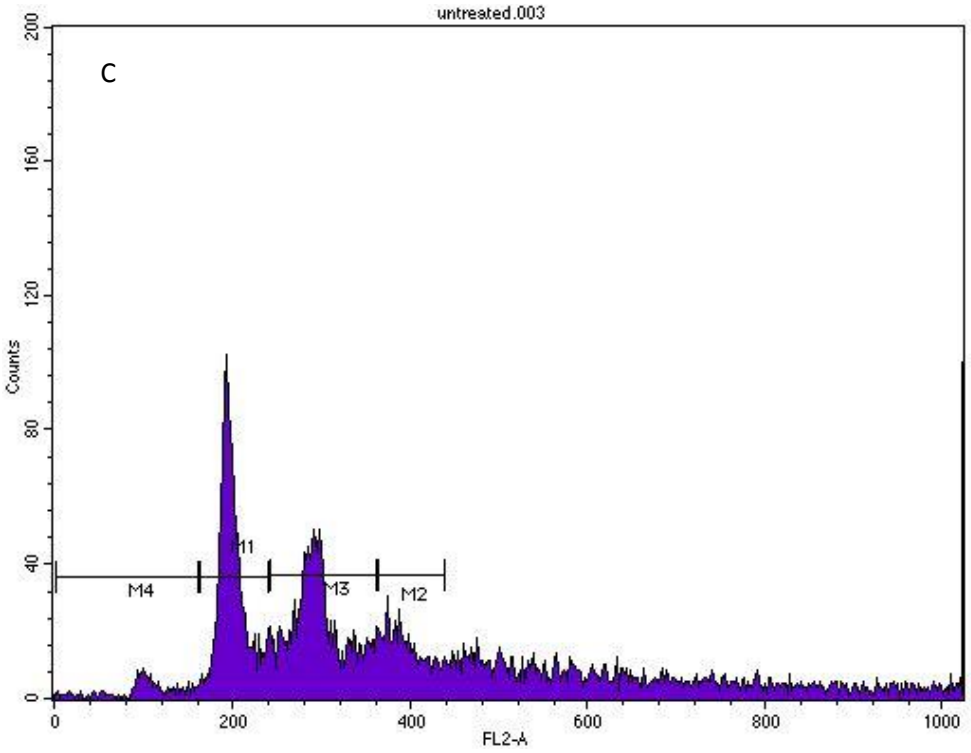

Figure S10C: Cell cycle of Untreated HeLa cells (Control).

We have quantified the nuclear and cytosolic distribution of **Rf@AuNPs** and **RfS@AuNPs** at each time point of the confocal images. We observe a preference of **RfS@AuNPs** for nuclear localization which peaks at 24 H time point, unlike **Rf@AuNPs**. The intensity of green color is found to be increased significantly from cytoplasm to nucleus with increasing incubation time as shown in Figure S11. However, the same phenomenon is not significant in case of **Rf@AuNPs** treatment (Figure S11).

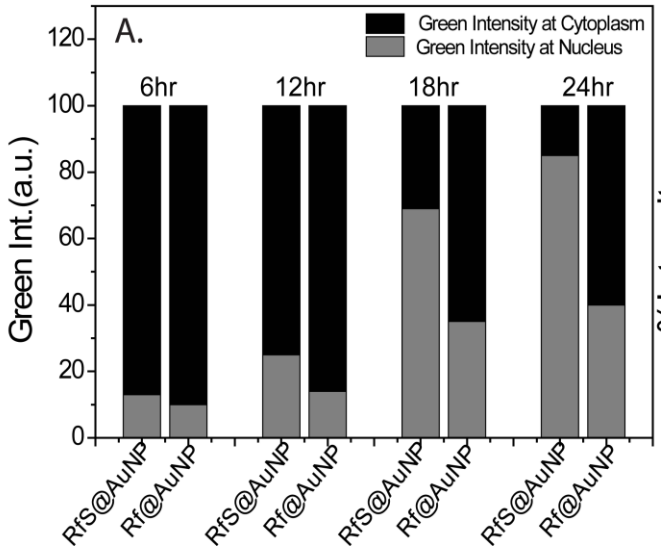

FigureS11: Relative green intensity within cytoplasm and nucleus for **RfS@AuNP** and **Rf@AuNP** (control) treated cells in different incubation time; [Intensity analysis is done based on the average of 4 cells' nucleus from each frame using 'Mathematica' software]

pH stability of RfS@AuNPs:

We are unable to check the pH stability of **RfS@AuNPs** within lysosomes and endosomes. However, we have performed stability assays of **RfS@AuNPs** at different pH employing fluorescence spectroscopy. The pH within the lysosome is around 5.0-5.5. Therefore, we have attempted to investigate the pH stability of **RfS@AuNPs** *in vitro*. The complex is dissolved in tris-buffer with pH 5.0, 7.2 and 8.5 and incubated for 12 H. Then, the resulting solutions are centrifuged at 4500 rpm for 2 H. The bottom part which contains **RfS@AuNPs** is collected and washed to remove free **RfSH** and resuspended into respective buffers. We have checked the corresponding fluorescence spectrum with the resuspended conjugates in buffer having three respective pH (Figure S12). If the nano conjugate becomes unstable in acidic pH, the intensity of the resuspended solution should decrease due to breaking of complexation from **AuNPs** with subsequent release of **RfSH** in the buffer before centrifugation. However, no such significant decrease in fluorescence intensity is observed in case of resuspended solution. The above experiment indicates that the nanoconjugate is quite stable at pH 5.0. Similar results may be obtained in lysosomal environment where pH is around 5.0. Moreover, the resuspended solutions with two other pH follow the same trend indicating that **RfS@AuNPs** is also stable at pH 7.2 and 8.5.

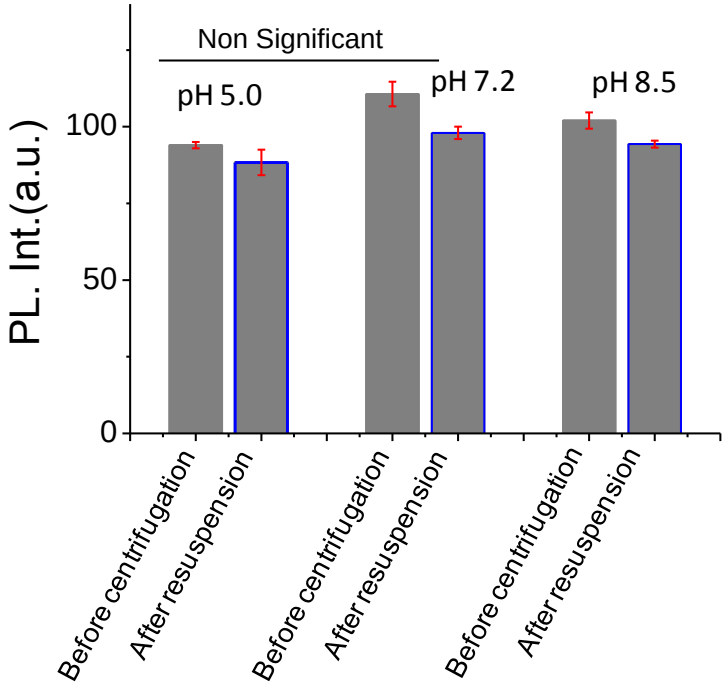

Figure S12: Relative fluorescence intensity of the **RfS@AuNPs** in tris buffer with different pH, 5.0, 7.2 and 8.5 before and after resuspension.

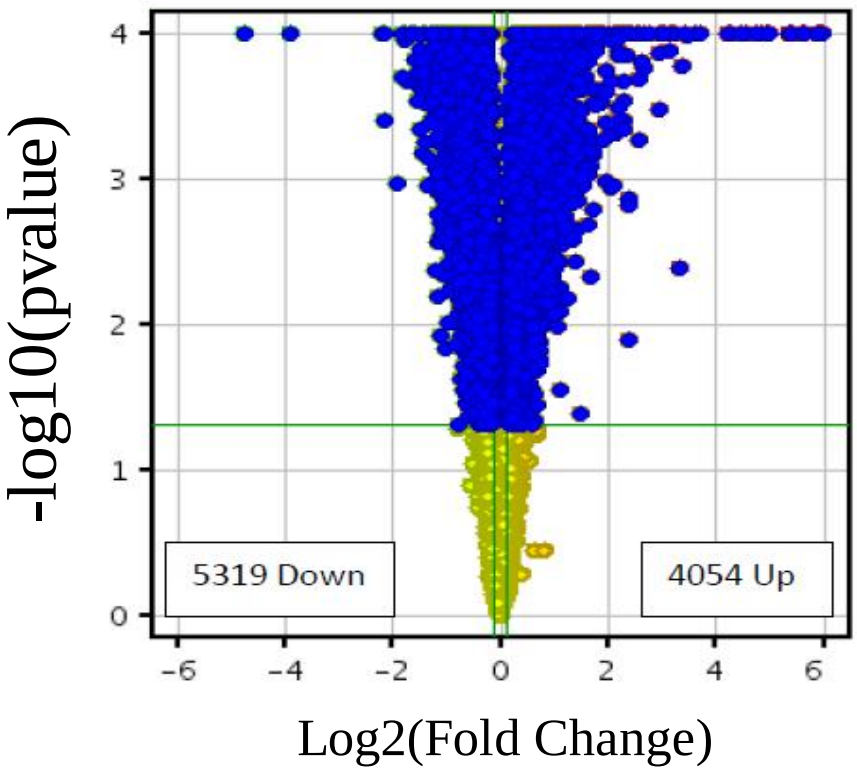

Figure S13: Volcano Plot: There are 9373 differentially expressed genes in **RfSH@AuNP** Treated *vs.* Control, where 4054 are Up regulated genes and 5319 are Down regulated genes at Fold change >=1.1 and P Value <=0.05.

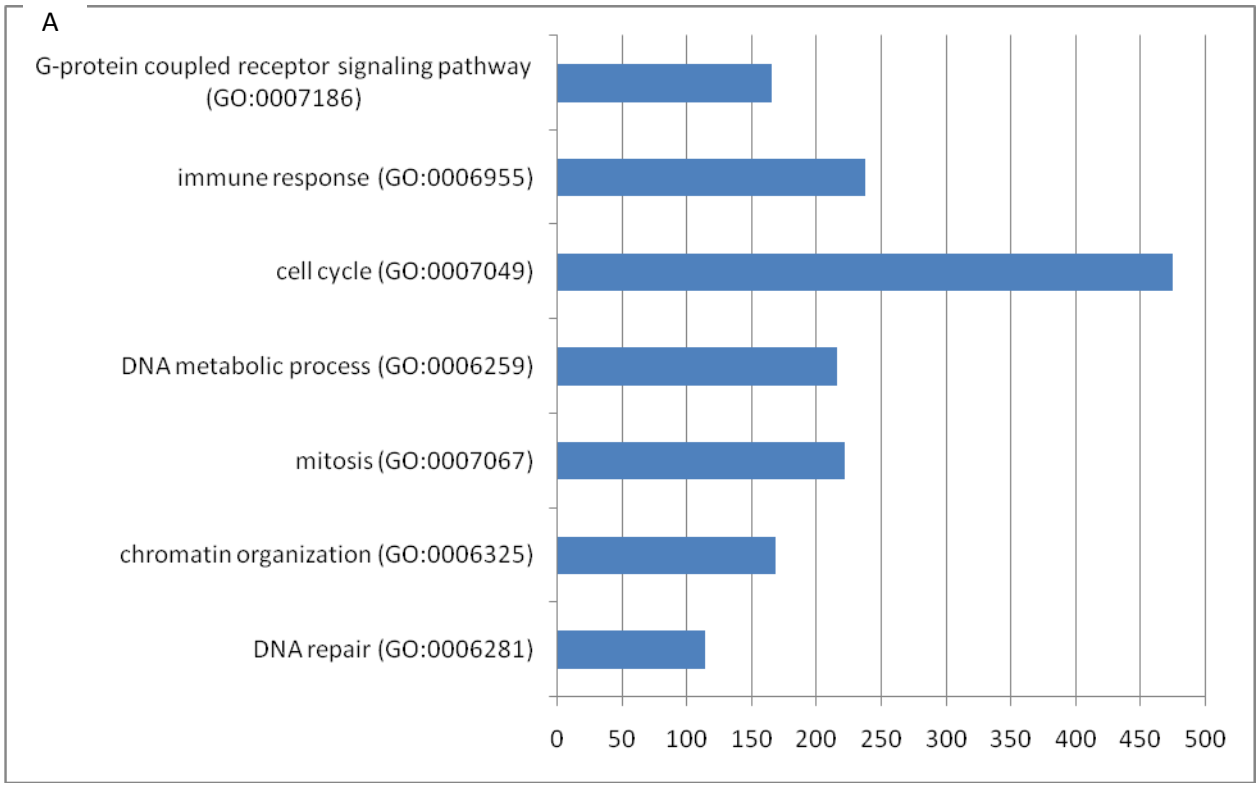
A
G-protein coupled receptor signaling pathway (GO:0007186)
immune response (GO:0006955)
cell cycle (GO:0007049)
DNA metabolic process (GO:0006259)
mitosis (GO:0007067)
chromatin organization (GO:0006325)
DNA repair (GO:0006281)
0 50 100 150 200 250 300 350 400 450 500

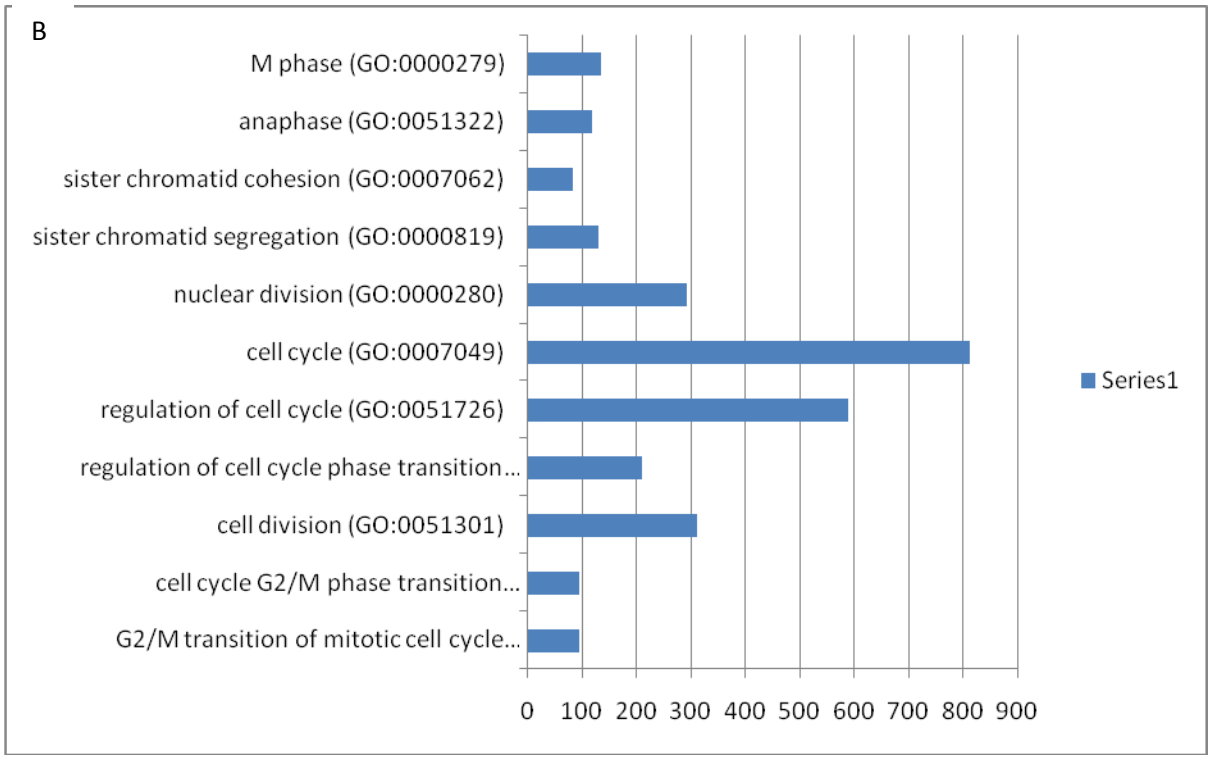
B
M phase (GO:0000279)
anaphase (GO:0051322)
sister chromatid cohesion (GO:0007062)
sister chromatid segregation (GO:0000819)
nuclear division (GO:0000280)
cell cycle (GO:0007049)
regulation of cell cycle (GO:0051726)
regulation of cell cycle phase transition...
cell division (GO:0051301)
cell cycle G2/M phase transition...
G2/M transition of mitotic cell cycle...
0 100 200 300 400 500 600 700 800 900
Series1

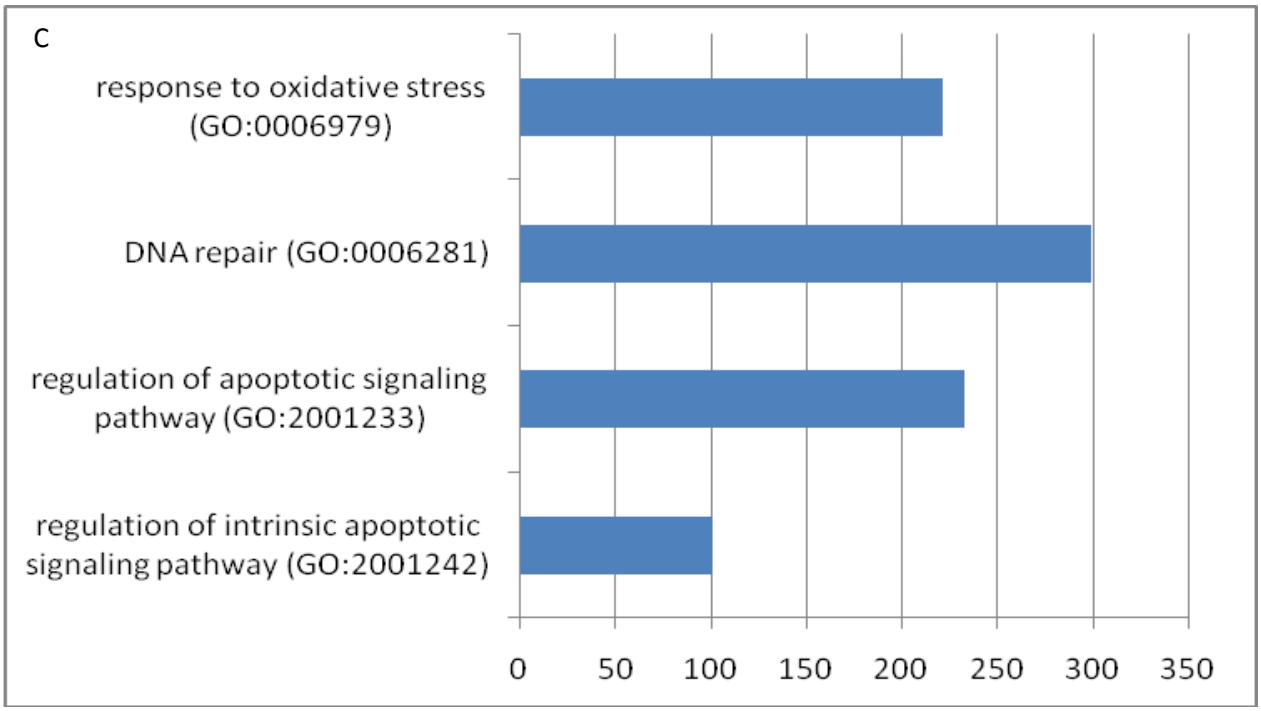

Figure S14: PANTHER analysis of cellular processes altered by **RfSH@AuNP** treatment. A and B. Gene Ontology (GO) analyses of changes in significant biological processes; (C) Significant changes in cell signaling pathways.